Fiber-array-based detection scheme for single-shot pulse contrast characterization

Dongfang Zhang,[1] Liejia Qian,[1,*] Peng Yuan,[1] Heyuan Zhu,[1] Shuangchun Wen,[1] and Chris Xu[2]

[1]*Department of Optical Science and Engineering, Laboratory for Advanced Materials, State Key Laboratory for Advanced Materials and Devices, Fudan University, Shanghai 200433, China*

[2]*School of Applied and Engineering Physics, Cornell University, Ithaca, New York 14853, USA*

**Corresponding author: ljqian@fudan.edu.cn*

Received June 6, 2008; accepted July 17, 2008;
posted July 29, 2008 (Doc. ID 97038); published August 25, 2008

We propose and demonstrate a fiber-array-based detection scheme for single-shot pulse contrast characterization. The parallel to serial mapping using the fiber array allows the use of a high-sensitivity photomultiplier tube and eliminates the external neutral density filter, both resulting in significantly improved dynamic range. The proof-of-principle experiments show a dynamic range of $2\times10^{7}:1$. The demonstrated technique can be readily applied to existing instruments for single-shot pulse characterization. © 2008 Optical Society of America

OCIS codes: 120.0120, 230.0040, 230.0230.

Focused intensity in excess of $10^{20}\ \mathrm{W/cm^2}$ now can be reached by high-power laser systems based on chirp pulse amplification [1–3], which may find many applications such as plasma physics, high-order harmonic generation, inertial confinement fusion, or quantum electrodynamics [4]. In the systems with such high intensities, however, reflections, scattering, amplified spontaneous emission, or incomplete temporal compression may result in considerable pedestal or prepulses and postpulses. The contrast, defined by the ratio of the peak intensity of the main pulse to its background, especially in the leading part, is therefore one of the most important parameters of a high-power laser pulse. For example, the absolute intensity of the long pedestal or prepulse must be under the threshold of preplasma generation for a clean light–matter interaction experiment. The higher the peak intensity, the higher the contrast is required. This, of course, necessitates a more delicate design of the laser system and/or pulses's cleaning techniques for higher peak intensity to meet the experimental criteria [5–7]. On the other hand, it also challenges the diagnostic technique for pulse contrast, which is necessary for experimental data analysis and system optimization.

Current diagnostic techniques for pulse contrast are typically based on nonlinear correlation, in which a clean reference is obtained by second-harmonic generation (SHG) of the to-be-characterized pulse. Sum-frequency generation (SFG) or difference-frequency generation (DFG) may serve as the nonlinear process for correlation, and the dependence of the third harmonics or the idler on temporal delay is measured to reveal the information of the shape and contrast of the primary pulse [8,9]. One of the most important specifications of such an instrument is its dynamic range, which determines the ability to distinguish the utmost difference of the signal levels. For a specific detection system the strongest signal detected must be kept below the saturation level, which is accomplished commonly by attenuation using a calibrated neutral density filter(s) [NDF(s)]. At the low end, the noise level sets the bottom limit of the detectable signal. The noise limit is indeed the most severe problem that restricts the obtainable dynamic range. Stray light suppression and using detectors with low noise and high sensitivity are thus preferable. In a time-scanning configuration for characterizing repetitive pulses, a lock-in amplifier or boxcar averager may be used to increase the dynamic range by 1–2 orders of magnitude [10,11]. In addition, a larger dynamic range could be achieved in principle by further increasing the intensity of the input beam while increasing the attenuation of the signal peak.

Although a dynamic range in excess of $10^{11}:1$ has been demonstrated for repetitive millijoule input pulses in a time-scanning mode [9], it is typically about $10^{6}-10^{7}:1$ for single-shot techniques [12–14]. In a single-shot measurement, which is especially desirable for high energy/high-power laser systems operating at extremely low repetition rate or even nonrepetitively, the information of the shape and contrast is obtained from an isolated pulse. Third-order autocorrelation based on SHG-SFG cascaded processes is widely used. Variation of the time delay is realized by intersecting the two interacting beams and/or tilting the pulses onto the SFG crystal [12], and the correlation in time is then transformed into a spatial intensity distribution. Currently the pulse correlation trace in a single-shot measurement is recorded by a multielement detector capable of parallel measurement such as a diode array. To increase the measurable contrast a calibrated attenuator is normally positioned to reduce the central portion of the signal while leaving the low-level pedestal unattenuated. The poorer dynamic range in a single-shot mode, when compared to that of a time-scanning mode, is largely due to the performance limits in its detection system. The attenuator for the central signal reduction, the width of which is narrower than that of the signal beam, will inevitably introduce extra noise through edge scattering or diffraction. Furthermore, the diode array for parallel measurement is much less sensitive than a photomultiplier tube (PMT) in a time-scanning setup, particularly when techniques for improving the signal-to-noise ratio, such as lock-in amplification or boxcar averaging, are precluded in a single-shot measurement. In this Letter, we report a fiber-array-based acquisition system for single-shot pulse contrast characterization. Our technique is designed to overcome some of the limitations of existing instruments. In particular, our technique eliminates the external NDF and allows a low-noise high-sensitivity PMT to accomplish the parallel measurement, achieving significantly improved dynamic range in a single-shot measurement.

The experimental setup is schematically shown in Fig. 1. In this proof-of-principle experiment we used the configuration of noncollinear DFG for the single-shot correlation measurement [15]. The output from a Ti:sapphire regenerative amplifier (Spitfire, Spectra-Physics) with a pulse energy of 400 μJ, duration of 70 fs, and wavelength of 800 nm was used as the initial source. After frequency doubling in a type I phase-matched 200 μm thick BiB_3O_6 (BIBO) crystal, a dichroic mirror separates the fundamental and second-harmonic components. These two components, after proper timing adjustment by an optical delay line, were focused by cylindrical lenses onto another type I phase-matched 200 μm thick BIBO crystal to produce a DFG signal. At the input face of the crystal the two beams overlap in an area of approximately 6 mm$\times$1 mm. The noncollinear angle was ~3° in the plane with the larger beam size (i.e., not focused by the cylindrical lens), which provided a temporal delay of ~2 ps across the beam. The spatially distributed DFG signal was then imaged by a cylindrical lens onto a well-aligned and end-polished fiber array. The fiber array consists of 61 fibers with different lengths, which was fabricated by a high precision V-groove-based technique (Broadex Technologies, China). Each fiber has a core diameter of 62.5 μm and an NA of 0.275, and the width of the array is ~7.75 mm. The fiber lengths range from ~1 m (the first fiber) to ~91 m (the 61st fiber), with a ~1.5 m increment between succesive fibers, which corresponds to a temporal interval of ~7.3 ns. Calibrated fiber attenuators were spliced into the central channels, with a fixed attenuation factor of 100 for fiber channels from the 27th to the 31st, and an attenuation factor of 32 for channels from the 24th to the 26th and from the 32nd to the 34th. The distal ends of the fibers were aligned and bound together. Thus, the spatially distributed DFG signal is converted into a series of temporally separated pulses spanning ~440 ns, and a serial instead of parallel detection can be used. In our experiments, an additional NDF with an attenuation factor of 50,000 was used to attenuate the overall intensity of the signal beam before reaching the detector. We note that the NDF can be eliminated simply by using fiber attenuators (variable type preferred) with much higher attenuation factors (e.g., up to 50–60 dB). A PMT (R5108, Hamamatsu) operating at −1260 V bias was used to capture the output light from the fiber bundle, the output of which was sent to an analog-to-digital converter followed by a personal computer for further data processing. The response time of ~1.2 ns of the PMT was fast enough to resolve the serially delivered DFG intensity profile because the designed temporal separation between two adjacent channels was sufficiently large (i.e., ~7.3 ns).

Figure 2 shows the retrieved shape of the fundamental pulse. The limit on the measurable contrast ratio was determined by optical noise level at the DFG wavelength (the fundamental wavelength in this case). The dominant noise source came from light scattered into the DFG signal from the fundamental beam. By blocking the second-harmonic beam the noise level was measured using data shown in Fig. 2. The measured optical noise was slightly nonuniform across the fiber array, which suggests that scattering of the fundamental beam may be nonuniformly distributed in both the spatial and angular domains. Although the pulse shape and the optical noise level were measured with different shots, it is reasonable to assume that variations for different shots are negligible owing to the high stability of the laser source used. The dynamic range under the present conditions was estimated to be 2×10^7:1. Because the DFG signal and the fundamental were degenerate the optical noise could not be eliminated fully in this specific configuration of a nonlinear pro-

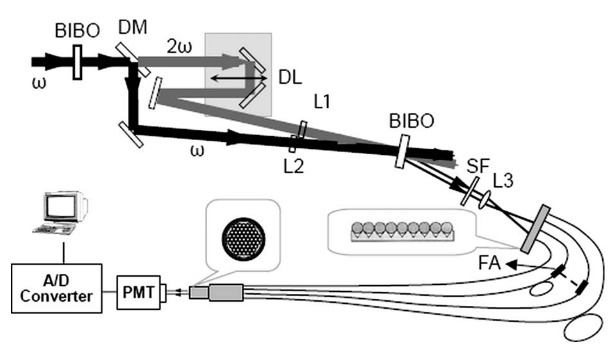

Fig. 1. Schematic of the measurement setup. DM, dichroic mirror; DL, optical delay line; L1 and L2, cylindrical lenses; SF, spectral filter; L3, imaging lens; FA, fiber attenuator.

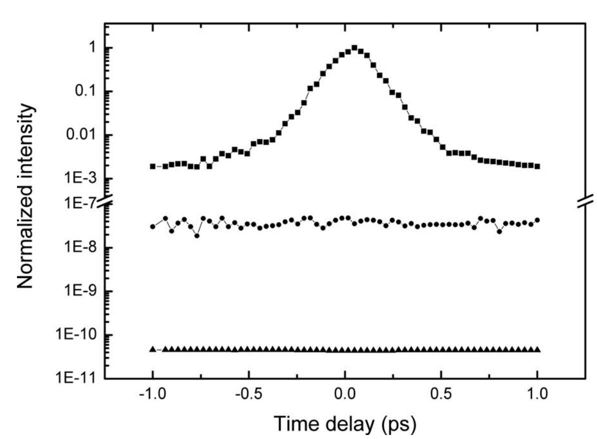

Fig. 2. Measured SHG–DFG correlation trace for the femtosecond Ti:sapphire laser (upper curve with square symbol). Measured optical noise resulted from the scattering at fundamental wavelength (middle curve with circle symbol), and electrical noise of PMT (bottom line with triangle symbol).

cess. Nonetheless, the fiber-array-based acquisition offers two additional advantages in reducing the optical noise: (1) the exclusion of a conventional external NDF avoided extra noise contribution and (2) each fiber itself acted as a spatial filter, which suppressed the scattering noise to some extent owing to its limited NA and core diameter. Because the optical noise overwhelmed the electrical noise of the detector by about 3 orders of magnitude, as shown by Fig. 2, the advantage of the high sensitivity of the PMT itself was not fully exploited in the present experiments. Higher dynamic range can be achieved if a nondegenerate scheme, e.g., third-harmonic generation (THG), is used where spectral filtration can be applied to further suppress the scattering from both the fundamental and second-harmonic components. THG was not conducted in this proof-of-concept experiment mainly owing to the lack of ultraviolet optics in our lab.

To examine the packaging uniformity and alignment of the proximal ends of the fibers we translated the fiber array transversely by ten channels to capture the DFG intensity profile by other shot. The comparison results are shown in Fig. 3. The consistency of the two traces clearly manifests the satisfactory uniformity of the fiber array and the shot-to-shot stability of the laser source as well. Finally, we note that the exact length increments between successive fibers are not important, provided that the increments are large enough to be resolved. Absolute length increments are automatically retrieved from the time domain serial data.

In conclusion, we have demonstrated what we believe to be a new detection scheme for single-shot pulse contrast characterization. The fiber-array-based scheme eliminates the NDF necessary in the conventional method while allowing a high-sensitivity PMT instead of the multielement photodiode array. The parallel to serial mapping by the fiber array forms a measurement configuration that is similar to the time-scanning mode except for the pulse averaging. The proof-of-principle experiments have shown a dynamic range of $2\times10^7:1$ with submillijoule pulse energy in a SHG–DFG configuration, and a higher dynamic range can be anticipated if the SHG–SFG configuration is used. Fabrication of broader fiber arrays (i.e., with more fiber channels) can be readily achieved using the V-groove-based technique. Thus, a larger temporal window of characterization may be accessible by increasing the widths of the interacting beams or pulse tilting for picosecond pulses. In practical applications, variable fiber attenuators can be used to provide a graded attenuation profile to accommodate different pulse shapes and contrasts. The NDF–diode array combination used in the existing instruments can be readily replaced by the proposed scheme to improve the dynamic range.

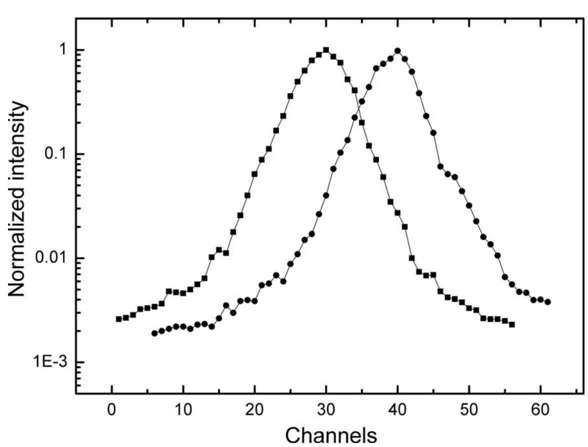

Fig. 3. Measured SHG–DFG correlation traces before and after transversely shifting the fiber array by ten channels

This work was partially supported by the National Natural Science Foundation of China (NNSFC) (grants 10576009, 60538010, and 60725418) and National Basic Research Program of China (973 Program) (grant 2007CB815104). C. Xu acknowledges the support from State Key Laboratory for Advanced Materials and Devices, Fudan University.

References

1. M. Pittman, S. Ferré, J. P. Rousseau, L. Notebaert, J. P. Chambaret, and G. Chériaux, Appl. Phys. B **74**, 529 (2002).
2. M. Aoyama, K. Yamakawa, Y. Akahane, J. Ma, N. Inoue, H. Ueda, and H. Kiriyama, Opt. Lett. **28**, 1594 (2003).
3. M. D. Perry, D. Pennington, B. C. Stuart, G. Tietbohl, J. A. Britten, C. Brown, S. Herman, B. Golick, M. Kartz, J. Miller, H. T. Powell, M. Vergino, and V. Yanovsky, Opt. Lett. **24**, 160 (1999).
4. G. A. Mourou, C. P. J. Barty, and M. D. Perry, Phys. Today **51**, 22 (1998).
5. Y. Beaudoin, C. Y. Chien, J. S. Coe, J. L. Tapié, and G. Mourou, Opt. Lett. **17**, 865 (1992).
6. K. Yamakawa, H. Shiraga, Y. Kato, and C. P. J. Barty, Opt. Lett. **16**, 1593 (1991).
7. H. Kiriyama, M. Mori, Y. Nakai, T. Shimomura, M. Tanoue, A. Akutsu, S. Kondo, S. Kanazawa, H. Okada, T. Motomura, H. Daido, T. Kimura, and T. Tajima, Opt. Lett. **33**, 645 (2008).
8. S. Luan, M. H. R. Hutchinson, R. A. Smith, and F. Zhou, Meas. Sci. Technol. **4**, 1426 (1993).
9. E. J. Divall and I. N. Ross, Opt. Lett. **29**, 2273 (2004).
10. P. F. Curley, G. Darpentigny, G. Cheriaux, J. P. Chambaret, and A. Antonetti, Opt. Commun. **120**, 71 (1995).
11. J. Collier, D. Hitchcock, C. Danson, and K. Weingarten, in *CLF Annual Report 190* (Rutherford Appleton Laboratory, 1996/97).
12. P. Pax, J. Weston, and W. E. White, Proc. SPIE **1229**, 82 (1990).
13. V. Sirutkaitis, R. Grigonis, A. Piskarskas, A. Persson, and S. Svanberg, Lith. J. Phys. **38**, 79 (1998).
14. J. Collier, C. Hernandez-Gomez, R. Allott, C. Danson, and A. Hill, Laser Part. Beams **19**, 231 (2001).
15. G. Priebe, K. A. Janulewicz, V. I. Redkorechev, J. Tümmler, and P. V. Nichles, Opt. Commun. **259**, 848 (2006).